

Nonequilibrium frequency-dependent noise through a quantum dot: A real-time functional renormalization group approach

C. P. Moca,^{1,2} P. Simon,³ C. H. Chung,⁴ and G. Zaránd¹

¹*Institute of Physics, Budapest University of Technology and Economics, H-1521 Budapest, Hungary*

²*Department of Physics, University of Oradea, 410087, Oradea, Romania*

³*Laboratoire de Physique des Solides, Univ. Paris Sud, CNRS, UMR 8502, F-91405 Orsay Cedex, France*

⁴*Electrophysics Department, National Chiao-Tung University, HsinChu, Taiwan, R.O.C.*

(Received 4 March 2011; published 10 May 2011)

We construct a real time current-conserving functional renormalization group (RG) scheme on the Keldysh contour to study frequency-dependent transport and noise through a quantum dot in the local moment regime. We find that the current vertex develops a nontrivial nonlocal structure in time that is governed by a new set of RG equations. Solving these RG equations, we compute the complete frequency and temperature dependence of the noise spectrum. For voltages that are large compared to the Kondo temperature (i.e., $eV \gg k_B T_K$), two sharp antiresonances are found in the noise spectrum at frequencies $\hbar\omega = \pm eV$ and, correspondingly, two Kondo-assisted peaks appear in the ac conductance through the dot.

DOI: [10.1103/PhysRevB.83.201303](https://doi.org/10.1103/PhysRevB.83.201303)

PACS number(s): 73.63.Kv, 72.15.Qm, 72.70.+m

Introduction. Not only the current flowing through a system, but also its fluctuations (noise), carry crucial information on the physics that governs transport.¹ Zero-frequency noise (shot noise) has been used; for example, to reveal the fractional charge of the quasiparticle excitations in a fractional quantum Hall liquid.² The low-frequency electrical noise has been extensively studied in various systems³ and is by now relatively well understood. However, even more information is stored in the finite-frequency (FF) current noise. It has been predicted that the FF noise is sensitive to the statistics of the quasiparticles⁴ and that in a quantum Hall liquid a crossover between different quantum statistics can be potentially observed as a function of frequency, similar to the one observed as a function of temperature.⁵ Moreover, in the quantum regime characterized by frequencies higher than the applied voltage or temperature, the FF noise is a powerful tool to reveal the characteristic time scales of the probed system⁶ as well as the dynamics of the excitations or the importance of interactions.

Quantum dots (QD) provide an ideal test ground to study nonequilibrium transport in the presence of strong interactions. Due to their small size, transport through quantum dots is strongly influenced by the Coulomb blockade. In particular, QDs with an odd number of electrons behave as artificial magnetic impurities and exhibit the Kondo effect,⁷ a paradigmatic many-body phenomenon corresponding to the screening of the spin of the quantum dot by the conduction electrons of the leads at temperatures T below the Kondo temperature T_K . While the conductance of a QD in the Kondo regime is well understood by now,⁸ much less is known about current fluctuations. Although noise is a promising quantity to characterize the out-of-equilibrium Kondo effect, nevertheless, most experiments have focused so far on measurements of the average current,^{9–11} and even results on low-frequency noise measurements have only appeared recently.^{12,13} While the effect of ac voltage on the nonequilibrium Kondo effect has been experimentally studied relatively long ago,¹⁴ to our knowledge no FF noise measurements have yet been reported. Also theoretically, most studies focused so far on shot noise:

a non monotonous bias-dependence of the shot noise with a maximum at $eV \sim k_B T_K$ has been found at $T \ll T_K$,¹⁵ and a universal ratio $(5/3)e$ between the shot noise and the backscattering current at $T = 0$ has been predicted for the SU(2) Kondo effect.¹⁶

The purpose of this work is to provide a general analysis of the finite-frequency current noise through a quantum dot in the local moment regime. To achieve this, we construct a real time functional renormalization group (FRG) scheme on the Keldysh contour to study frequency-dependent transport and noise through a Kondo quantum dot. Our formalism sums up the leading logarithmic singularities just as Abrikosov's parquet approximation,¹⁷ and reproduces the scaling equations of Rosch *et al.*¹⁸ for the vertex function. However, we find that the current vertex also develops a nontrivial nonlocal structure in time governed by a new set of RG equations. Such a structure of the current vertex turns out to be unavoidable to guarantee current conservation and is necessary to calculate the finite-frequency current noise in a controlled manner. Solving this set of RG equations, we compute the complete frequency- and temperature-dependent noise spectrum through the dot. Our approach is valid at any frequency ω , voltage V , and temperature T provided that $\max\{eV, k_B T\} > k_B T_K$. For frequencies $\hbar\omega \gg k_B T_K$, we find sharp antiresonances in the voltage dependence of the noise spectrum at $eV = \hbar\omega$, which gradually disappear with increasing temperature and which can be understood as Kondo-assisted noise singularities. The absorption noise is also found to exhibit strong anomalies at $\hbar\omega = eV$, and we find similar anomalies in the nonequilibrium ac conductance, too, where a split nonequilibrium Kondo resonance is observed. Precursors of the noise anomaly have been found in the zero-temperature symmetrized noise at finite frequency, as first computed at the Toulouse point of the Kondo model¹⁹ and later confirmed by a nonequilibrium one-loop perturbative calculation.²⁰ However, logarithmic singularities are completely absent at the rather special Toulouse point,¹⁹ while the method of Ref. 20 was not accurate enough to capture fine details of the anomaly.

Theoretical Model. In this paper, we focus our attention to the local moment regime of the quantum dot, where we can describe the electron on the dot as a spin $S = 1/2$ moment which couples to electrons in the left and right electrodes through the exchange interaction⁸

$$H_{\text{int}} = \frac{1}{2} \sum_{\alpha, \beta=L, R} \sum_{\sigma, \sigma'} j_{\alpha\beta} \mathbf{S} \psi_{\alpha\sigma}^\dagger \boldsymbol{\sigma}_{\sigma\sigma'} \psi_{\beta\sigma'}. \quad (1)$$

Here $\boldsymbol{\sigma}$ stands for the three Pauli matrices, the fields $\psi_{\alpha\sigma} = \int c_{\alpha\sigma}(\xi) e^{-i\xi|a} d\xi$ destroy electrons of spin σ in leads $\alpha \in \{L, R\}$, with $1/a$ being a high energy cutoff.²¹ Here the dynamics of $\psi_{\alpha\sigma}$ are governed by the noninteracting Hamiltonian $H_0 = \sum_{\alpha, \sigma} \int d\xi (\xi + \mu_\alpha) c_{\alpha\sigma}^\dagger(\xi) c_{\alpha\sigma}(\xi)$, where $\mu_\alpha = eV_\alpha$ is the chemical potential shift of lead α and ξ is the electrons' energy in the leads.

To describe the spin using standard field-theoretical methods, we make use of Abrikosov's pseudo-fermion representation:¹⁷ we introduce a fermion operator f_s^\dagger for each spin component $s = \pm 1/2$ and represent the spin operator as $\hat{S}^i \rightarrow \sum_{s, s'} \frac{1}{2} f_s^\dagger \sigma_{s, s'}^i f_{s'}$ with the additional constraint $\sum_s f_s^\dagger f_s = 1$.

We then employ a path integral formalism on the Keldysh contour. In this approach each fermionic field is replaced by two time-dependent Grassmann fields living on the upper and lower Keldysh contour ($\kappa = 1, 2$), respectively, and the dynamics are determined by the Keldysh action, $\mathcal{S} = \mathcal{S}_{\text{lead}} + \mathcal{S}_{\text{spin}} + \mathcal{S}_{\text{int}}$. The parts $\mathcal{S}_{\text{lead}}$ and $\mathcal{S}_{\text{spin}}$ describe the conduction electrons and the spin in the absence of interaction. They are quadratic in the fields and determine the noninteracting Green's functions.²²

The interaction part of the action, \mathcal{S}_{int} , is diagonal in the Keldysh indices and is initially local in time. However, elimination of high-energy degrees of freedom in the course of the RG procedure generates retardation effects, and the interaction becomes nonlocal. We find that, with a good approximation, it can be expressed as

$$\mathcal{S}_{\text{int}} = \sum_{\kappa} \sum_{\alpha, \beta} s_{\kappa} \frac{1}{4} \int dt_1 dt_2 g_{\alpha\beta}(t_1 - t_2) \times \bar{f}^{\kappa}(T_{12}) \vec{\sigma} f^{\kappa}(T_{12}) \cdot \bar{\psi}_{\alpha}^{\kappa}(t_1) \vec{\sigma} \psi_{\beta}^{\kappa}(t_2), \quad (2)$$

where $T_{12} = (t_1 + t_2)/2$ and $s_{\kappa} = \pm 1$ for the upper and lower Keldysh contours, respectively. The initial (bare) coupling function $g_{\alpha\beta}(t)$ is local in time and is given by $g_{\alpha\beta}^{(0)}(t) = j_{\alpha\beta} \delta(t)$. The justification for this structure, Eq. (2), is straightforward: At electronic time scales the spin evolves very slowly, and its time evolution can be very well approximated by the one in the absence of interactions. However, conduction electrons have fast dynamics and their retardation effects become important as one approaches smaller energy scales.

Functional Renormalization Group. We construct the RG equations by expanding the action in \mathcal{S}_{int} and rescaling the cutoff parameter $a \rightarrow a'$. An integro-differential equation is obtained for the functions $g_{\alpha\beta}(t)$, which becomes simple in Fourier space:

$$\frac{d\mathbf{g}(\omega)}{dl} = \mathbf{g}(\omega) \mathbf{q}(\omega, a) \mathbf{g}(\omega). \quad (3)$$

Here $l = \ln(a/a_0)$ is the scaling variable, a_0 is the initial value of the cutoff time, and we introduced the matrix notation

$g_{\alpha\beta} \rightarrow \mathbf{g}$. The matrix $\mathbf{q}(\omega, a)$ is a cutoff function, which depends somewhat on the precise cutoff scheme but, for practical purposes, it is well approximated by the function $q_{\alpha\beta}(\omega, a) \approx \delta_{\alpha\beta} \Theta(\frac{1}{a} - |\omega - \mu_\alpha|)$ at temperature $T = 0$.¹⁸ The scaling equation, Eq. (3), is identical to the one obtained in a more heuristic way in Ref. 18; however, in our real time functional RG formalism the derivation is rather straightforward and simple.²³ We remark that the usual poor man's RG procedure can be recovered by dropping the time dependence of $g_{\alpha\beta}$ and replacing the generated nonlocal couplings by local ones, $g_{\alpha\beta}(t) \rightarrow \delta(t) \int dt g_{\alpha\beta}(t)$, which corresponds to setting $\omega \rightarrow 0$ in Eq. (3).

Our primary purpose is to compute current-current correlation functions. To do that, we first define the left and right current operators from the equation of motion as $\hat{I}_L(t) = -\hat{I}_R(t) = \sum_{\alpha\beta} \frac{e}{2} v_{\alpha\beta}^L \hat{\mathbf{S}}(t) \cdot \hat{\psi}_{\alpha}^{\dagger}(t) \boldsymbol{\sigma} \hat{\psi}_{\beta}(t)$, with the current vertex matrices defined as

$$\mathbf{v}^L = -\mathbf{v}^R = \begin{pmatrix} 0 & -ij_{LR} \\ ij_{LR} & 0 \end{pmatrix}. \quad (4)$$

In the path integral language, it is useful to introduce a corresponding generating functional,

$$Z[h_{\alpha}^{\kappa}(t)] \equiv \langle e^{-i \sum_{\kappa, \alpha} \int dt h_{\alpha}^{\kappa}(t) I_{\alpha}^{\kappa}(t)} \rangle_{\mathcal{S}}, \quad (5)$$

from which the current-current correlation functions can be generated by functional differentiation with respect to $h_{\alpha}^{\kappa}(t)$. A systematic investigation of the leading logarithmic diagram series shows that the expression of the current field $I^{\kappa}(t)$ necessarily becomes nonlocal in time under the RG procedure and acquires the form (no summation over κ)

$$I_L^{\kappa}(t) = \frac{e}{4} \sum_{\alpha\beta} \int dt_1 dt_2 v_{\alpha\beta}^L(t_1 - t, t - t_2, a) \times \bar{f}^{\kappa}(t) \vec{\sigma} f^{\kappa}(t) \cdot \bar{\psi}_{\alpha}^{\kappa}(t_1) \vec{\sigma} \psi_{\beta}^{\kappa}(t_2). \quad (6)$$

The physical motivation of the double time structure is simple: in the renormalized theory it is not enough to know the times at which electrons enter and leave the dot ($t_{1,2}$), but the time t of the current measurement must also be kept track of.

It is relatively straightforward to derive the scaling equations from the perturbative expansion of Eq. (5). We obtain

$$\frac{d\mathbf{V}^L(\omega_1, \omega_2)}{dl} = \mathbf{V}^L(\omega_1, \omega_2) \mathbf{q}(\omega_2, a) \mathbf{g}(\omega_2) + \mathbf{g}(\omega_1) \mathbf{q}(\omega_1, a) \mathbf{V}^L(\omega_1, \omega_2). \quad (7)$$

This equation needs be solved parallel to the scaling equation, Eq. (3), with the boundary conditions $\mathbf{V}^L(\omega_1, \omega_2, a_0) = \mathbf{v}^L(\tau_1, \tau_2, a_0) = \delta(\tau_1) \delta(\tau_2) \mathbf{v}^L$ and $\mathbf{V}^R(\tau_1, \tau_2, a_0) = \delta(\tau_1) \delta(\tau_2) \mathbf{v}^R$. Although the renormalized couplings $\mathbf{g}_L(\omega)$ drive the scaling of the current vertices $\mathbf{V}_L(\omega_1, \omega_2, a_0)$, there seems to be no simple connection between these two. In other words, introducing the renormalized current vertices within the functional RG scheme is unavoidable to compute time-dependent current correlations. The above extension also seems to be necessary to guarantee current conservation. Equation (7) is linear in \mathbf{V}^L and, therefore, the condition $I_L^{\kappa}(t) + I_R^{\kappa}(t) \equiv 0$ is automatically satisfied for any value a of the cutoff. On the other hand, we could not find any way to generate a current field from just the renormalized action, Eq. (2), such that it respects current conservation.

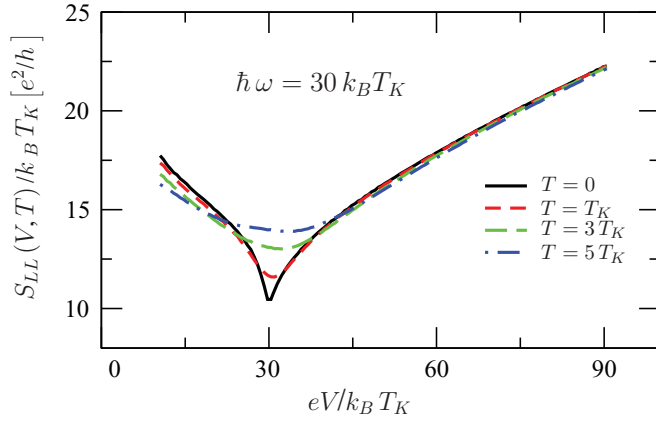


FIG. 1. (Color online) Voltage dependence of the symmetric noise as computed by FRG for $\hbar\omega = 30k_B T_K$.

We solved Eqs. (3) and (7) numerically to obtain \mathbf{g} , \mathbf{V}^L , and \mathbf{V}^R . All of them display singularities at frequencies $\hbar\omega = \pm eV/2$.²² With the couplings $\mathbf{g}(\omega_1)$ and the current vertices $\mathbf{V}^L(\omega_1, \omega_2)$ and $\mathbf{V}^R(\omega_1, \omega_2)$ in hand, we then proceeded to compute the noise through the device by doing perturbation theory with the renormalized action. For the Fourier transform of the absorption and emission noise components, $S_{LL}^>(t) \equiv \langle \hat{I}_L(t) \hat{I}_L(0) \rangle$ and $S_{LL}^<(t) \equiv \langle \hat{I}_L(0) \hat{I}_L(t) \rangle$, respectively, we obtain $S_{LL}^>(\omega) = S_{LL}^<(-\omega)$, with

$$S_{LL}^>(\omega) = \frac{e^2}{2} S(S+1) \int \frac{d\tilde{\omega}}{2\pi} \text{Tr} \{ \mathbf{V}^L(\tilde{\omega}_-, \tilde{\omega}_+) \times \mathbf{G}^>(\tilde{\omega}_+) \mathbf{V}^L(\tilde{\omega}_+, \tilde{\omega}_-) \mathbf{G}^<(\tilde{\omega}_-) \}. \quad (8)$$

Here, $\tilde{\omega}_\pm = \tilde{\omega} \pm \frac{\omega}{2}$, and the greater and lesser Green's functions are $G_{\alpha\beta}^>/<(\omega) = \pm i2\pi \delta_{\alpha\beta} f(\pm(\omega - \mu_\alpha))$, respectively.

Results. The symmetrized noise spectrum, $S_{LL}(\omega) \equiv \frac{1}{2}[S_{LL}^>(\omega) + S_{LL}^<(\omega)]$ is plotted in Fig. 1 for $\hbar\omega = 30k_B T_K$ as a function of voltage V . Clearly, the noise spectrum shows rather strong features at the bias voltage $eV \approx \hbar\omega$. The appearing dip is a clear fingerprint of the nonequilibrium Kondo effect; It gradually vanishes as we increase the temperature T .²⁴ The origin of this anomaly can be better understood by

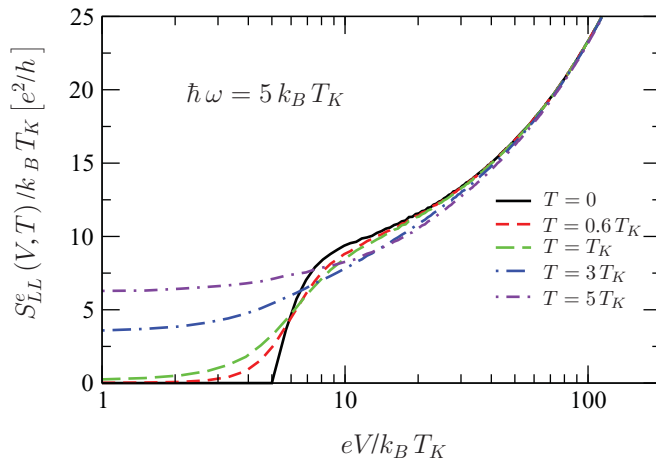


FIG. 2. (Color online) Voltage and temperature dependence of the emission noise as computed through FRG for $\hbar\omega = 5k_B T_K$.

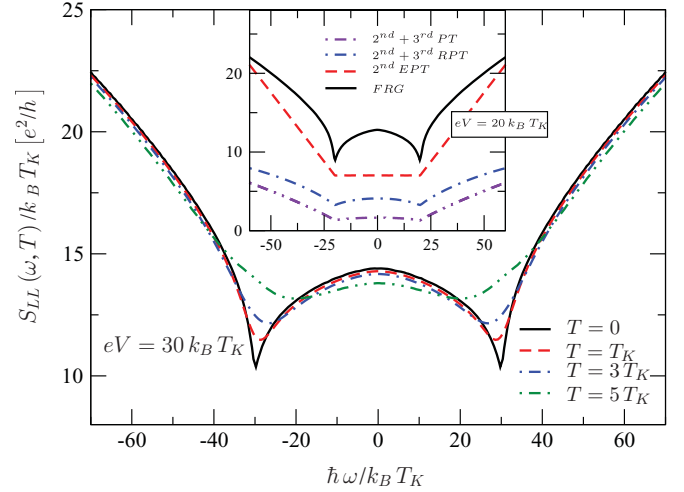


FIG. 3. (Color online) Temperature dependence of the symmetric noise, as computed by FRG for $T_K = 6.3 \times 10^{-5} \hbar/a_0$. Inset: Comparison with third-order bare perturbation theory (PT) and renormalized perturbation theory (RPT) using a reduced cutoff, $\tilde{a} = \hbar/(10eV)$ and the corresponding couplings $j_{LR}(\tilde{a})$ and effective second-order perturbation theory (EPT) with renormalized couplings $j_{LR}(\tilde{a} = \hbar/(eV))$, but still using the original bandwidth. None of these methods are able to get close to the FRG results.

analyzing the emission (or absorption) noise, $S_{\alpha\beta}^{e/a}(\omega > 0) \equiv S_{\alpha\beta}^<(\pm\omega)$, as a function of the bias voltage (see Fig. 2). In fact, it turns out to be more convenient experimentally to measure these quantities.²³ The emission noise vanishes for voltages $V < \hbar\omega/e$ at $T = 0$ by energy conservation. However, for $eV > \hbar\omega$, photon emission becomes possible through processes where an electron is transferred through the dot. These processes have a logarithmic singularity (cut off by the voltage-induced spin relaxation rate) since, for $\hbar\omega \approx eV$, the initial and final electron states are very close to the Fermi energies of the corresponding leads. Correspondingly, the slope of S^e at the threshold is very large due to the nonequilibrium Kondo effect, while it becomes smaller as one goes away from the threshold. A similar anomaly appears in the absorption noise for $eV < \hbar\omega$. These Kondo-assisted emission and absorption noises give rise to a sharp dip in

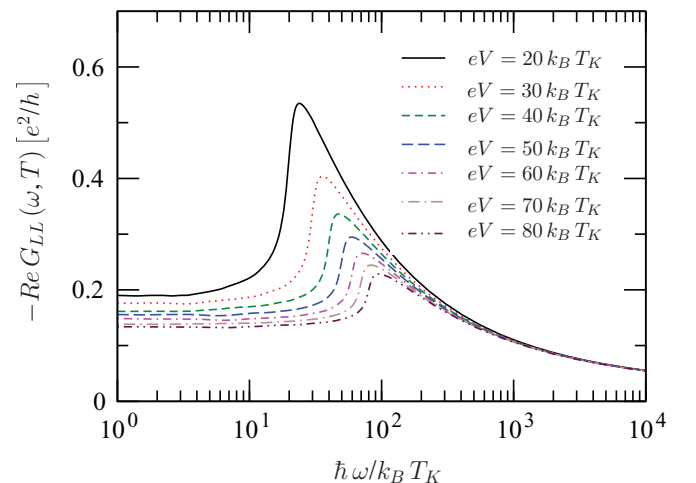


FIG. 4. (Color online) Ac conductance for $\omega > 0$ and $T = 0$.

the symmetrized noise at temperatures $T \ll T_K$, which is gradually smeared out for $k_B T > eV$ (see Fig. 1). The increase in the symmetrized noise with decreasing V at low voltages has a different origin; it is the consequence of increasing spin relaxation time, giving rise to an increased Kondo conductance through the dot. At very high voltages, on the other hand, the increasing noise is associated with increased photon emission.

Similar Kondo-effect-induced features appear in the frequency-dependent symmetrized noise shown in Fig. 3. It is instructive to compare the FRG results with perturbation theory, which gives

$$S_{LL}^>(t) = -e^2 \frac{3}{4} |j_{LR}|^2 \cos(eVt) \times \left\{ \frac{1}{(t-ia)^2} + 2(j_{LL} + j_{RR}) \frac{\ln(1+it/a)}{t(t-2ia)} + \dots \right\}. \quad (9)$$

The curves in the inset of Fig. 3 were obtained by taking the Fourier transform of this expression. While the perturbative result also exhibits singular features at $\hbar\omega = \pm eV$, it does not reproduce the precise shape of the anomaly, even if we use renormalized parameters, $j_{\alpha\beta} \rightarrow j_{\alpha\beta}(eV)$, obtained by solving the usual leading logarithmic scaling equations.

Finally, let us discuss another quantity of experimental relevance; the nonequilibrium finite-frequency linear conductance, which is defined as the current response of the system to an external time-dependent variation of one of the lead potentials. According to a formula of Safi,²⁶ this can be expressed as

$$\text{Re } G_{LL}(\omega, V) = -\frac{1}{\hbar\omega} [S_{LL}^>(\omega) - S_{LL}^<(\omega)]. \quad (10)$$

Notice that $G_{LL}(0, V)$ is just the usual nonequilibrium differential conductance, $G_{LL}(0, V) = \partial_{V_L} \langle \hat{I}_L \rangle$, while $G_{LL}(\omega, V \rightarrow 0)$ corresponds to the usual equilibrium ac conductance.²⁷ $\text{Re } G_{LL}(\omega, V)$ is an even function of ω and exhibits two peaks at $\hbar\omega = \pm eV$, which are associated with the nonequilibrium Kondo effect¹⁵ (see Fig. 4). Since in equilibrium $G_{LL}(\omega, 0)$ is directly related to the spectral function of the dot level, this result suggests that the dips in the noise are related to the splitting of the Kondo resonance at a finite bias.²³

Summary. We have developed a real-time functional renormalization group approach. We have shown that the current vertex becomes nonlocal in time under renormalization, under renormalization. This nonlocal structure ensures nonequilibrium current conservation. We have been able to calculate the voltage and temperature dependence of the current noise at finite frequency and the nonequilibrium ac conductance; quantities which are within experimental reach.²⁵

Acknowledgments. We would like to thank J. Basset, R. Deblock, H. Bouchiat, and B. Reulet for interesting discussions. This research has been supported by Hungarian grants No. OTKA K73361 and TAMOP-4.2.1/B-09/1/KMR-2010-0002, No. K73361, Romanian grant CNCSIS PN II ID-672/2008, the EU GEOMDISS project, Taiwan's NSC grants No. 98-2918-I-009-06 and No. 98-2112-M-009-010-MY3, the MOE-ATU program, and the NCTS of Taiwan, R.O.C. C. H. C. acknowledges the hospitality of Yale University.

¹R. Landauer, *Nature (London)* **392**, 658 (1998).

²L. Saminadayar, D. C. Glattli, Y. Jin, and B. Etienne, *Phys. Rev. Lett.* **79**, 2526 (1997).

³Ya. M. Blanter and M. Büttiker, *Phys. Rep.* **336**, 1 (2000).

⁴I. Safi, P. Devillard, and T. Martin, *Phys. Rev. Lett.* **86**, 4628 (2001); S. Vishveshwara, *ibid.* **91**, 196803 (2003); C. Bena and C. Nayak, *Phys. Rev. B* **73**, 155335 (2006).

⁵A. Bid, N. Ofek, M. Heiblum, V. Umansky, and D. Mahalu, *Phys. Rev. Lett.* **103**, 236802 (2009).

⁶J. Gabelli and B. Reulet, *Phys. Rev. Lett.* **100**, 026601 (2008).

⁷D. Goldhaber-Gordon, Hadas Shtrikman, D. Mahalu, David Abusch-Magder, U. Meirav, and M. A. Kastner, *Nature* **391**, 156 (1998); S. M. Cronenwett, Tjerk H. Oosterkamp, and Leo P. Kouwenhoven, *Science* **24**, 540 (1998).

⁸L. I. Glazman and M. Pustilnik, in *Lectures notes of the Les Houches Summer School 2004 in "Nanophysics: Coherence and Transport,"* edited by H. Bouchiat *et al.* (Elsevier, 2005), pp. 427–478.

⁹S. DeFranceschi, R. Hanson, W. G. van der Wiel, J. M. Elzerman, J. J. Wijkema, T. Fujisawa, S. Tarucha, and L. P. Kouwenhoven, *Phys. Rev. Lett.* **89**, 156801 (2002).

¹⁰J. Paaske, A. Rosch, P. Wölfle, N. Mason, C. M. Marcus, and J. Nygård, *Nature Phys.* **2**, 460 (2006).

¹¹M. Grobis, I. G. Rau, R. M. Potok, H. Shtrikman, and D. Goldhaber-Gordon, *Phys. Rev. Lett.* **100**, 246601 (2008).

¹²T. Delattre C. Feuillet-Palma, L. G. Herrmann, P. Morfin, J.-M. Berroir, G. Fève, B. Plaçais, D. C. Glattli, M.-S. Choi, C. Mora, and T. Kontos, *Nature Phys.* **5**, 208 (2009).

¹³O. Zarchin, M. Zaffalon, M. Heiblum, D. Mahalu, and V. Umansky, *Phys. Rev. B* **77**, 241303 (2008).

¹⁴A. Kogan, S. Amasha, and M. A. Kastner, *Science* **304**, 1293 (2004).

¹⁵Y. Meir and A. Golub, *Phys. Rev. Lett.* **88**, 116802 (2002).

¹⁶E. Sela, Y. Oreg, F. von Oppen, and J. Koch, *Phys. Rev. Lett.* **97**, 086601 (2006); A. O. Gogolin and A. Komnik, *ibid.* **97**, 016602 (2006).

¹⁷A. A. Abrikosov, *Physics* **2**, 5 (1965).

¹⁸A. Rosch, J. Kroha, and P. Wölfle, *Phys. Rev. Lett.* **87**, 156802 (2001); A. Rosch, J. Paaske, J. Kroha, and P. Wölfle, *ibid.* **90**, 076804 (2003).

¹⁹A. Schiller and S. Hershfield, *Phys. Rev. B* **58**, 14978 (1998).

²⁰T. Korb, F. Reininghaus, H. Schoeller, and J. König, *Phys. Rev. B* **76**, 165316 (2007).

²¹The operators $c_{\alpha\sigma}(\xi)$ satisfy the anticommutation relation $\{c_{\alpha\sigma}^\dagger(\xi), c_{\alpha'\sigma'}(\xi')\} = \delta_{\alpha\alpha'} \delta_{\sigma\sigma'} \delta(\xi - \xi')$.

²²See supplemental material at [<http://link.aps.org/supplemental/10.1103/PhysRevB.83.201303>].

²³C. P. Moca *et al.* (unpublished).

²⁴Finite temperature has been included through the spin relaxation time, similar to Ref. 18.

²⁵J. Basset, H. Bouchiat, and R. Deblock, *Phys. Rev. Lett.* **105**, 166801 (2010).

²⁶I. Safi, arXiv:0908.4382 [see also I. Safi, C. Bena, and A. Crépieux, *Phys. Rev. B* **78**, 205422 (2008)].

²⁷M. Sindel, W. Hofstetter, J. von Delft, and M. Kindermann, *Phys. Rev. Lett.* **94**, 196602 (2005).